Original Article

DOI: 10.5582/bst.2022.01281

Hepatic stellate cell exosome-derived circWDR25 promotes the progression of hepatocellular carcinoma *via* the miRNA-4474-3P-ALOX-15 and EMT axes

Lei Liu[1,2,§], Rui Liao[1,§,*], Zhongjun Wu[1,§], Chengyou Du[1,§], Yu You[3,4,§], Keting Que[3,4], Yuxin Duan[1], Kunli Yin[1], Wentao Ye[1]

[1] Department of Hepatobiliary Surgery, the First Affiliated Hospital of Chongqing Medical University, Chongqing, China;
[2] Department of Hepatobiliary Surgery, the People's Hospital of Yubei District of Chongqing City, Chongqing, China;
[3] Chongqing Key Laboratory of Hepatobiliary Surgery, The Second Affiliated Hospital of Chongqing Medical University, Chongqing, China;
[4] Department of Hepatobiliary Surgery, the Second Affiliated Hospital of Chongqing Medical University, Chongqing, China.

SUMMARY Recently, the emerging role of circular RNAs (circRNAs) in tumor development and progression has been a topic of great interest. Nevertheless, the effects of hepatic stellate cell (HSC)-derived exosomes in hepatocellular carcinoma (HCC) remain unclear. Here, we aim to explore the potential effect of HSC exosome-derived circWDR25 on the aggressiveness of HCC. Firstly, a microarray analysis of circRNAs was performed to profile and identify the differentially expressed circRNAs derived from HSC exosomes activated by HCC cells. Subsequently, the roles of circWDR25 in HCC tumor growth and aggressiveness were confirmed through *in vitro* and *in vivo* functional experiments. Moreover, RNA pull-down, dual-luciferase reporter assays, and fluorescent in situ hybridization (FISH) were performed to determine interactions in the circWDR25-miR-4474-3p-ALOX15 loop. Immunohistochemical analysis was also performed on a microarray of HCC tissues and peritumoral tissues. We found that overexpressed peritumoral circWDR25 was associated with survival and recurrence in patients with HCC and promoted the progression of HCC cells both *in vitro* and *in vivo*. Mechanistically, both exogenous and HSC exosomal-derived circWDR25 regulated the expression of ALOX15 by sponging miR-4474-3p and ultimately inducing an epithelial-to-mesenchymal transition (EMT) in HCC cells. Moreover, exogenous and HSC exosomal-derived circWDR25 promoted the expression of CTLA-4 in HSCs and PD-L1 in HCC cells. In conclusion, circWDR25 facilitated HCC cell proliferation and invasion *via* the circWDR25/miR-4474-3p/ALOX15 and EMT axes and it promoted the expression of CTLA-4 in HSCs and PD-L1 in HCC cells, thus providing insights into the mechanism of tumor aggressiveness mediated by HSC-derived exosomal circWDR25.

Keywords liver cancer, mesenchymal cells, extracellular vesicles, circular RNA, prognosis

1. Introduction

Hepatocellular carcinoma (HCC) is one of the most malignant tumors, accounting for approximately 90% of all cases of primary liver cancer, and it is gradually becoming the second deadliest tumor globally (*1-3*). Although rational approaches to the diagnosis and treatment of HCC have been developed, the long-term outcomes are unfortunately still generally poor due to its high metastatic ability as well as its high recurrence rate (*4-6*). Thus, understanding the molecular mechanisms of HCC, and especially the inflammatory/immune response or genetic regulatory networks in HCC microenvironments, is of paramount importance.

During HCC progression, activated hepatic stellate cells (HSCs) are thought to accelerate hepatocarcinogenesis by producing extracellular matrix proteins and inflammatory cytokines (*7*). Current studies have revealed the potential mechanisms involving activated HSCs driving hepatocarcinogenesis by affecting cell autophagy (*8*), proliferation (*9*), migration and invasion (*10*), and tumor angiogenesis (*11*). The current authors previously reported that the secretion of HSCs, such as IF-6-, TNF-α-, and TREM-1-mediated crosstalk with hepatoma cells, induces a fertile environment favoring HCC (*12-14*). That said, the current authors also found that the balancing relationship between HSCs and different infiltrating lymphocytes (*e.g.*, Th17 cells (*15*)

and γδT cells (*16*)) contributes to the aggressiveness and recurrence of HCC. However, the crucial role of HSCs in dictating the immunologic reaction to the tumor in an immunosuppressive network is still unclear.

Exosomes, a subset of small extracellular vesicles (EVs) with an average size of 100 nm (range: 40-160 nm), are important media for intercellular communication (*17*). Recently, a vast array of studies have suggested that in various tumor types, tumor-derived exosomes play an important role in information transmission between tumor cells and the corresponding microenvironment during tumor progression (*18,19*). In addition, exosomes derived from other different types of cells, such as macrophages (*20*), mast cells (*21*), fibroblasts (*22*), and mesenchymal stem cells (*23*), mediate bidirectional crosstalk with tumor cells. In HCC, tumor-derived exosomes have the power to activate HSCs by triggering Hedgehog (*24*) and PDK1/AKT signalling (*25*) to promote tumor progression. However, the roles of HSC-derived exosomes in tumor cells and the molecular mechanisms of exosomal HSCs in the oncogenesis and development of HCC are still unknown.

Circular RNAs (circRNAs) are newly classified endogenously expressed regulatory noncoding RNA (ncRNA) members with a single-stranded circular structure that contribute to cell growth, angiogenesis, unlimited replicative potential, and cancer development by sponging different miRNA sequesters (*26*). Mounting evidence corroborates the fact that circRNAs induce aberrant functions in the HCC tumor microenvironment and mediate tumor biology. For instance, circPABPC1 can inhibit tumor cell adhesion and migration by downregulating ITGB1 (β_1 integrin) in HCC (*27*). Intriguingly, a recent study revealed that circPSD3 inhibited the activation and proliferation of HSCs and subsequently alleviated hepatic fibrogenesis (*28*). However, the underlying function and mechanism of HSC exosome-derived circRNAs in cancer remain elusive.

Based on a microarray analysis of circRNA, the current study identified an HSC-derived exosomal oncogenic circRNA, termed circWDR25. Moreover, the current authors found that a high level of expression of peritumoral circWDR25 was associated with a poor prognosis for patients with HCC. Moreover, circWDR25 sponges miR-4474-3p to upregulate ALOX15 expression. Exogenous circWDR25 or HSC-derived exosomal circWDR25 promoted hepatoma cell proliferation, migration, and invasion and it induced EMT in hepatoma cells. Significantly, the current authors found that HSC-derived exosomal circWDR25 participated in the immune response in HCC microenvironments by increasing PD-L1 expression in hepatoma cells and CTLA-4 expression in activated HSCs. To the extent known, this study is the first to demonstrate that HSC-derived exosomal circWDR25 and its downstream target gene miR-4474-3p/ALOX15 play a considerable role in HCC progression and to provide novel potential targets and approaches for treating HCC.

2. Materials and Methods

2.1. Patients and specimens

All archival specimens were obtained from 348 patients who were pathologically confirmed to have HCC after R0 curative hepatectomy from January 2011 to December 2014. None of the patients had received prior anticancer therapy or had other malignancies. All patients were followed up until June 2021. This study was specifically approved by the Ethics Review Committee of the First Hospital Affiliated with Chongqing Medical University, and written informed consent was obtained from all participants.

2.2. Tissue microarray design, immunohistochemistry, and H&E staining

A tissue microarray (TMA) was constructed as described previously (*14*). Immunohistochemistry (IHC) was performed according to the manufacturer's instructions (Invitrogen, Zymed Polymer Detection System). Positively stained cells were observed under high-power magnification (400×).

2.3. Survival and correlation analysis

Recurrence-free survival (RFS) and overall survival (OS) in patients with HCC were analyzed using Kaplan-Meier's method and the log-rank test. A multivariate Cox proportional hazards regression model was used to identify independent prognostic factors. Correlations between circWDR25, miR-4474-3p, and ALOX15 expression and various clinicopathological or serological variables were analyzed using the Mann-Whitney *U* test.

2.4. Cell lines and transfection of lentiviral vectors

The human HCC cell lines SMMC-7721, hep3B (Academy of Life Sciences of Chongqing Medical University) and HCCLM3 (Liver Cancer Institute, Zhongshan Hospital) were cultured in Dulbecco's modified Eagle's medium (DMEM) supplemented with 10% foetal bovine serum and 1% penicillin/streptomycin. In some experiments, to detect the effects of ALOX15 on the expression of PD-L1 in HCC cells, HCC cells were cultured in the presence of 1 μmol/mL or 10 μmol/mL ALOX15 inhibitors (PD146176, MedChemExpress, USA) for 24 h. In some experiments, to assess the expression of CTLA-4 in HSCs, HSCs were cultured 10 ng/mL or 100 ng/mL LPS (L2880, Sigma-Aldrich) for 24 h.

A lentiviral vector for circWDR25-overexpression

(circWDR25OE) or a lentiviral vector containing shRNA-circWDR25 to knockdown circWDR25 (circWDR25KD), and miR-44474-3p mimics were synthesized (Shanghai Genechem Co. Ltd., Shanghai, China). Stable transfectants were characterized using a quantitative real-time polymerase chain reaction (qRT–PCR).

2.5. Isolation and identification of exosomes

The culture medium of HSCs was collected. Isolation of exosomes from HSCs in all experiments was performed by ultracentrifugation as described previously with minor modifications (*29*). Briefly, supernatant fractions were collected from HSC cell cultures by centrifugation at 500 g for 5 min. The supernatant was centrifuged at 2,000 g for 10 min, and then the supernatant was collected and centrifuged at 10,000 g for 30 min again. Exosomes were then centrifuged at 100,000 g for 70 min to remove shed microvesicles. The supernatant was filtered with a 0.22-μm membrane filter (Merck Millipore). Finally, the exosome pellet was resuspended in 10 ml of PBS and collected by ultracentrifugation at 100,000 g for 70 min. Then, the exosome size and particle number were analyzed and verified using a DS500 nanoparticle characterization system (NanoSight) and electron microscopy.

In some experiments, before isolation of exosomes, HSCs were transfected with circWDR25KD or circWDR25OE lentivirus or a blank vector (circWDR25NC) in order to obtain HSC exosome-derived circWDR25KD or circWDR25OE.

2.6. Microarray analysis of circRNA

Total RNA was extracted from HSC-derived exosomes for microarray analysis (untreated HSC-derived exosomes and HSC-derived exosomes cocultured with three HCC cell lines). The labelled circRNAs were hybridized onto an Arraystar Human circRNA Array V2 (8 × 15K, Arraystar) based on the manufacturer's standard protocol. circRNAs that were significantly differentially expressed in two samples were identified through fold-change filtering ≥ 2.0 and a p value of < 0.05.

2.7. In situ hybridization and fluorescence in situ hybridization (FISH) testing

TMAs were dewaxed and rehydrated. Then, 3% hydrogen peroxide was used to treat the slices for 10 minutes to inactivate endogenous enzymes. Proteinase K was applied to the slices to expose nucleic acid segments at 37°C for 30 minutes. After prehybridization at 37°C for 2 h, TMAs were hybridized with specific DIG-labelled probes at 37°C overnight. After blocking, biotinylated anti-digoxin was added to the slices for reaction at 37°C for 1 h. After washing, the slides were reacted with streptavidin-biotin complex peroxidase at 37°C for 30 minutes and stained with DAB and hematoxylin. The method for counting positive cells was the same as that for IHC. The procedures for the FISH assay were similar to those for the ISH assay except that specific FAM-labelled circWDR25 probes and Cy3-labelled miR-4474-3p probes were used and stained with DAPI. Slides were photographed under a fluorescence microscope. The probe sequences are shown in Table S1 (*http://www.biosciencetrends.com/action/getSupplementalData.php?ID=107*).

2.8. Dual-luciferase reporter gene detection assay

A luciferase reporter plasmid was generated using a Mutagenesis Kit (QIAGEN, California, USA). The targeted sequence (wild type) of ALOX15 or circWDR25 was added downstream of firefly luciferase; Renilla luciferase was used as an internal reference. The mutant reporter was also used as a control. After cotransfection with the reporter plasmid and miR-4474-3p mimics or an inhibitor or NC oligos, 293T cells were cultured in 96-well plates for 48 h. Finally, the cells were extracted, and firefly and Renilla luciferase activity was quantified with a dual-luciferase reporter assay (Promega, USA).

2.9. RNA pull-down assay

A circWDR25 probe was designed and synthesized (Shanghai Genechem Co. Ltd., Shanghai, China). Hep3B cells were harvested and lysed. M280 streptavidin Dynabeads (Invitrogen) were incubated with the circWDR25 probe to generate probe-coated beads, which were incubated with the cell lysates at 4°C overnight. Then, the RNA complexes bound to the beads were eluted and extracted with a RNeasy Mini Kit (Qiagen) for qRT-PCR analysis.

2.10. qRT-PCR

Total RNA was isolated using TRIzol Reagent (Life Technologies, Carlsbad, CA, USA) according to the manufacturer's instructions. The qRT-PCR primer sequences are provided in Table S1 (*http://www.biosciencetrends.com/action/getSupplementalData.php?ID=107*).

2.11. Western blotting

The proteins were electrophoresed using SDS-containing polyacrylamide gels, transferred onto polyvinylidene fluoride (PVDF) membranes (Millipore Corp., Billerica, MA, USA), and blocked with 5% nonfat dry milk in 0.1% Tween (TBST) buffer at room temperature for 2 h. The membranes were incubated at 4°C overnight with the appropriate primary antibody. Antibodies were detected

using HRP-conjugated secondary antibody (Abcam) for 2 h at room temperature. All of the antibodies used in this study are listed in Table S2 (*http://www.biosciencetrends.com/action/getSupplementalData.php?ID=107*).

2.12. Cell proliferation, migration, and Matrigel invasion assays

Cell proliferation was measured using the Cell Counting Kit 8 (CCK-8, Dojindo, Japan) assay as described previously (*30*). A total of 5×10^3 cells were maintained in 96-well plates. At 0, 24, 48 and 72 h after treatment, cell viability was measured.

As described previously (*13*), for transwell migration assays, HCC cells were prestarved for 24 h prior to running the assay, and HCC cells (1×10^5/well) in serum-free medium were placed in an 8-μm pore upper chamber (24-well insert, Millipore, USA). Complete medium was added to the lower chambers. For invasion assays, HCC cells (1×10^5/well) were placed in the upper chamber with a Matrigel-coated membrane (BD, USA). After 24 h of incubation, cells were fixed with methanol and stained with crystal violet.

2.13. Wound healing assay

After incubation for 24 h, HCC cells were seeded and cultured in 6-well plates (1×10^6/well) to 90% confluence. Cell monolayers were scratched with a sterile 200-μL pipette tip to form a wound. Cell migration was quantified by measuring the relative area of the wound at 0, 24 and 48 h using inversion microscopy (Olympus, Japan).

2.14. Xenograft model

Balb/c-nude mice were purchased from the National Laboratory Animal Center (6-8 weeks old, Shanghai, China). As described previously (*31,32*), six mice per group were used for xenograft experiments, and cell suspensions in 100 μL phosphate-buffered saline (PBS) containing 1×10^7 HCC cells (SMMC-7721 and Hep3B) were injected subcutaneously into the right flank. Tumor growth was monitored and measured weekly, and tumor volume was calculated. Tumor bulk was calculated according to the following formula: volume = (width^2 × length)/2. When the tumors reached a volume of approximately 100 mm^3, the mice were randomly assigned to three groups, and mice with tumors were injected weekly with 100 μL of PBS at 5 μg per dose of HSC-derived exosomes with circWDR25 knockdown or blank vector for 4 weeks. Afterward, the animals were sacrificed. All animal care and experimental protocols were performed in line with the guidelines of the Animal Ethics Committee of Chongqing Medical University.

2.15. Statistical analysis

Values are expressed as the mean ± standard deviation (SD). Student's *t* test was used for comparisons between groups. Categorical data were analyzed using a chi-squared test and Fisher's exact probability test. Correlations between circWDR25, miR-4474-3p, and ALOX15 expression and various clinicopathological or serological variables were analyzed using the Mann-Whitney *U* test. RFS and OS in patients with HCC were analyzed using Kaplan-Meier's method and the log-rank test. A multivariate Cox proportional hazards regression model was used to identify independent prognostic factors. The "minimum *p* value" approach (*33*) was used to obtain an optimal cut-off for RFS.

3. Results

3.1. CircWDR25 is highly expressed in activated HSC exosomes induced by hepatoma cells

After coculturing with HCC cells (Figure 1A), HSC-derived exosomes were successfully isolated and identified using electron microscopy, a nanoparticle characterization system, and exosomal biomarkers (Figure 1B-D). According to circRNA microarray analysis, the levels of expression of various exosomal circRNAs from activated HSCs changed (Table S3, *http://www.biosciencetrends.com/action/getSupplementalData.php?ID=108*). Among the circRNAs that changed significantly (≥ 2-fold change and $p < 0.05$), 152, 145, and 124 circRNAs were upregulated and 144, 213, and 75 circRNAs were downregulated in HSC exosomes after stimulation with SMMC-7721, Hep3B, or HCCLM3 compared to untreated HCC cells (Figure 1E). Notably, hsa_circRNA_004310 (GeneSymbol: WDR25) was the most significantly and consistently upregulated exosomal circRNA in the HSC-derived exosomes cocultured with the three HCC cell lines (Figure 1F).

3.2. High levels of peritumoral circWDR25 and α-SMA expression correlate with a poor prognosis for patients with HCC

To further investigate the clinical relevance of circWDR25 and activated HSCs in patients with HCC, in situ hybridization (Figure 2A) was used to analyze the expression of circWDR25 and α-SMA (an activated HSC marker) in a TMA consisting of 348 HCC tissues. Interestingly, the levels of circWDR25 and α-SMA expression decreased significantly in peritumoral liver tissues compared to paired intratumoral tissues from the same patient (Figure S1, *http://www.biosciencetrends.com/action/getSupplementalData.php?ID=106*), and the expression was mainly localized in the cytoplasm. Kaplan-Meier survival analysis revealed that both intratumoral circWDR25 and intratumoral α-SMA could not predict outcomes for patients with HCC. However, levels of both peritumoral circWDR25 and

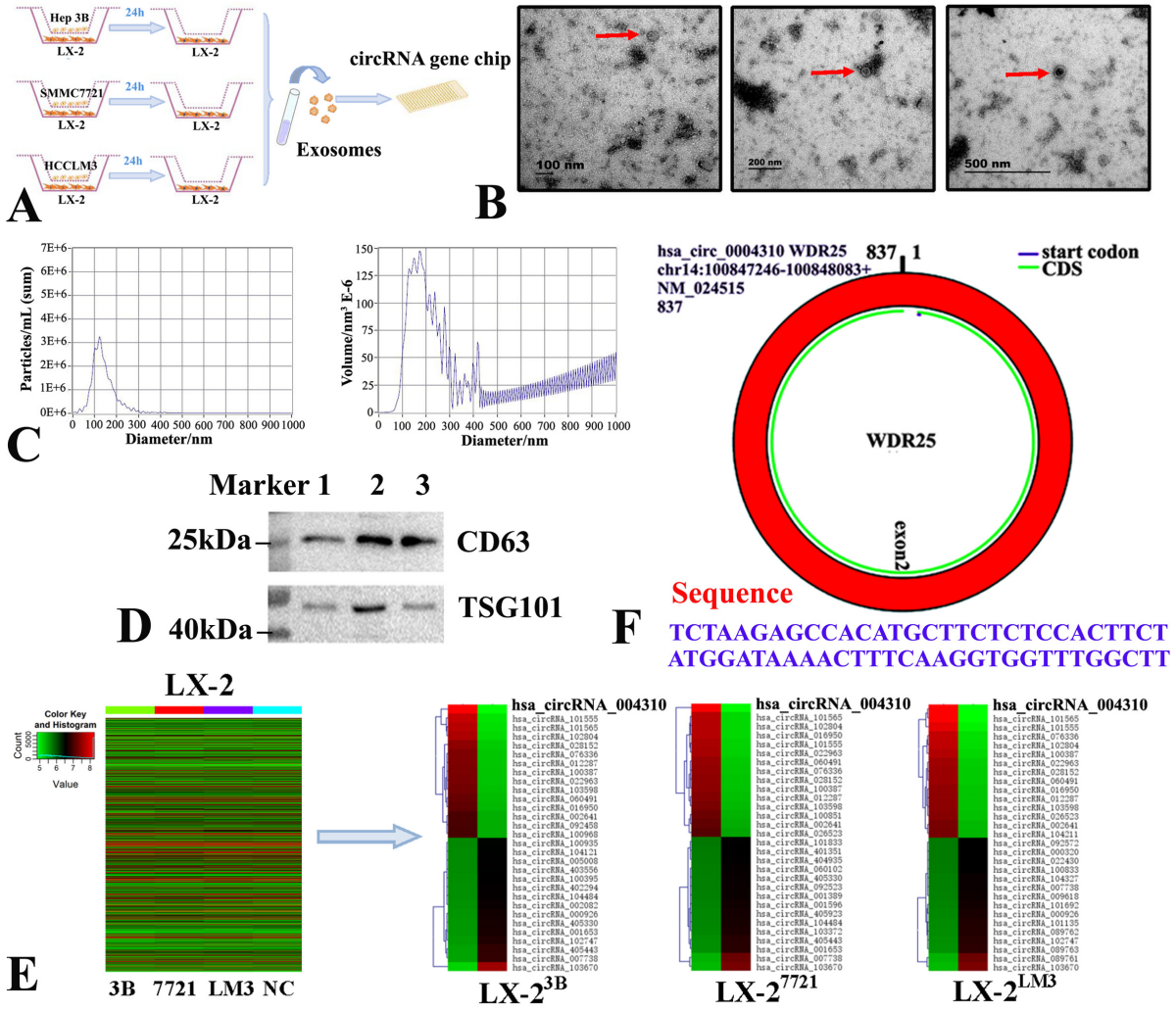

Figure 1. Identification of circWDR25 in hepatic stellated cell (HSC)-derived exosomes. A: Diagram showing the procedure to obtain HSC-derived exosomes for circRNA gene chip analyses. **B:** Transmission electron microscopy image of exosomes from HSCs indicated with red arrows. **C:** Nanoparticle tracking analysis of HSC-derived exosomes, confirming that more than 95% of the detected particles ranged in size from 30-200 nm in diameter. **D:** Exosome markers (CD63 and TSG101) in HSC-derived exosomes detected with Western blot analysis. **E:** Each panel of 2 separate LX-2 exosomes per group (LX-2 *vs*. LX-2 cocultured with the three HCC cell lines, respectively) displayed hierarchical clustering based on differential expression of circRNA genes represented as a heat map. **F:** Diagram of the genomic location of circWDR25 and the circularization of WDR25 exon 2 forming circWDR25.

peritumoral α-SMA expression were associated with OS and RFS. Patients with high levels of expression of both peritumoral circWDR25 and peritumoral α-SMA had a poorer prognosis (Figure 2B). Multivariate analysis indicated that both circWDR25 and α-SMA were independent predictors for OS and RFS in patients with HCC (Table S4, *http://www.biosciencetrends.com/action/getSupplementalData.php?ID=107*). Together, these results corroborated the circRNA microarray data, which revealed increased exosomal circWDR25 expression in tumor-activated HSCs. Moreover, these data indicated that elevated circWDR25 expression in HSC-derived exosomes may contribute to the progression of HCC.

Furthermore, a high level of expression of peritumoral circWDR25 was only significantly correlated with total bilirubin ($p = 0.038$). Patients with HCC and α-SMA overexpression had larger tumors ($p = 0.030$, Table S5, *http://www.biosciencetrends.com/action/getSupplementalData.php?ID=107*). The level of expression of peritumoral circWDR25 was positively correlated with that of peritumoral α-SMA ($r = 0.212$, $p < 0.001$; Figure 2C).

3.3. HSC exosome-derived circWDR25 promotes HCC tumor growth *in vivo* and *in vitro*

To investigate the biological functions of HSC exosome-derived circWDR25 in HCC, a lentiviral vector for circWDR25OE or a lentiviral vector containing circWDR25KD was successfully constructed to transfect HSCs (Figure 2D), and a xenograft mouse model was created (Figure 2E-F). The two HCC cell-induced tumors indicated that tumors implanted with HSC-derived exosomes had a larger tumor burden and grew faster than

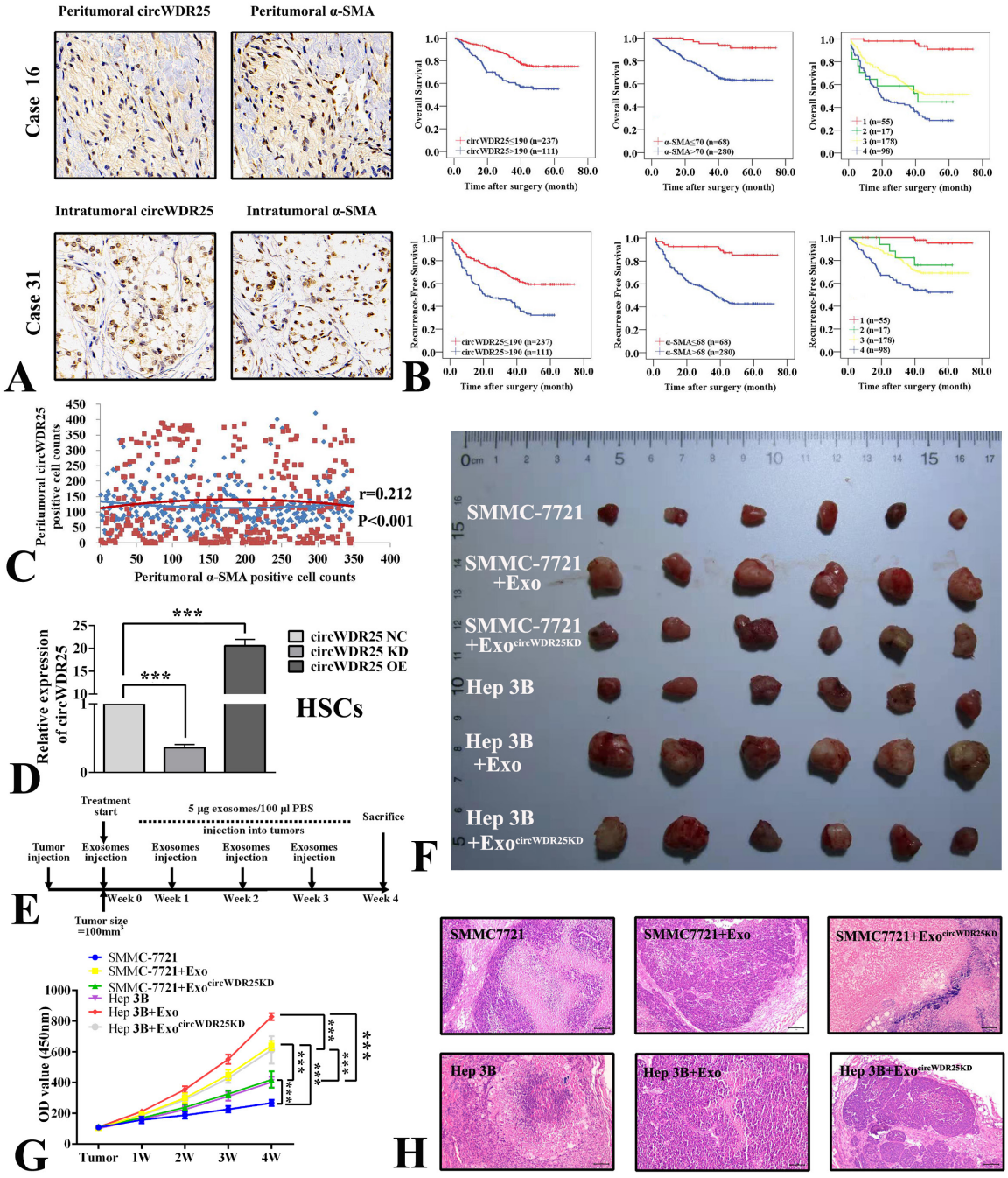

Figure 2. The expression and characterization of circWDR25 in HCC tissues from patients and xenograft mice. A: Consecutive sections were used to detect the expression of circWDR25 and α-SMA via in situ hybridization in 348 pairs of peritumoral and matched intratumoral HCC tissues (400× magnification). **B:** Peritumoral circWDR25, α-SMA, and a combination of the two were related to overall survival (OS) and recurrence-free survival (RFS) of patients with HCC after curative resection. **C:** The scatter diagram indicated that the expression of peritumoral circWDR25 is positively related to that of peritumoral α-SMA. **D:** A lentiviral vector for circWDR25OE or circWDR25KD was successfully constructed to transfect HSCs. **E:** Diagram of the procedure to establish a xenograft mouse model affected by HSC-derived exosomal circWDR25. **F:** Representative images of subcutaneous xenograft tumors treated or not treated with HSC-derived exosomal circWDR25 ($n = 6$ for each group). **G:** Growth curves for tumor volume, which was measured every week after injection of HSC-derived exosomes into the tumors. **H:** Representative H.E staining images of mouse tumors (100× magnification). All data are expressed as the mean ± SD of three independent experiments, $^{***}p < 0.001$.

those injected with circWDR25KD transported by HSC-derived exosomes or a blank vector without exosomes (Figure 2G-H).

In *in vitro* experiments, exosomes were isolated from HSCs with circWDR25OE or circWDR25KD or with a blank lentiviral vector (circWDR25NC). After coculturing with HSC-derived exosomes, the efficiency and specificity of circWDR25 overexpression and knockdown in HCC cells (SMMC-7721 and Hep3B) were verified using qRT–PCR (Figure 3A). Subsequent CCK-8 assays, transwell assays, and wound healing assays were performed to assess proliferation,

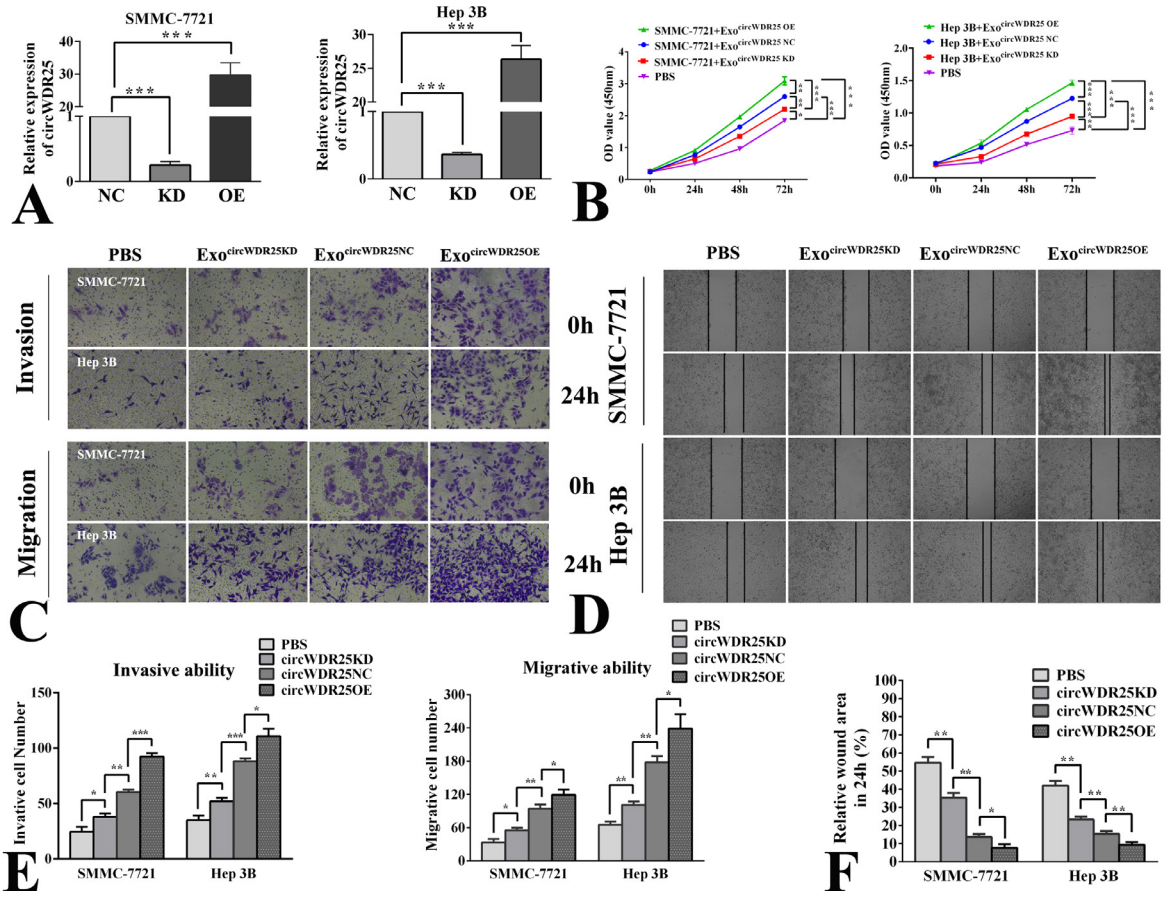

Figure 3. HSC exosome-derived circWDR25 promotes proliferation, migration, and invasion by HCC cells *in vitro*. A: Relative circWDR25 expression in HCC cell lines was determined with qRT-PCR after coculturing with HSC exosome-derived circWDR25KD, circWDR25OE, or circWDR25NC. **B:** The growth curves for HCC cells were assessed using CCK-8 assays after coculturing with HSC exosome-derived circWDR25KD, circWDR25OE, or circWDR25NC. **C:** Transwell assays were performed to evaluate migration and invasion by HCC cells. **D:** A wound healing assay wase performed to assess cell migration. **E:** Numbers of invading and migrating cells according to a transwell assay. **F:** Relative wound area based on the wound healing assay. All data are expressed as the mean ± SD of three independent experiments. $^{*}p < 0.05$, $^{**}p < 0.01$, $^{***}p < 0.001$.

migration, and invasion by HCC cells as were affected by HSC-derived exosomes (Figure 3B-D). The CCK-8 assay indicated that HSC-derived exosomes with circWDR25OE markedly increased the proliferation of HCC cells, while HSC-derived exosomes with circWDR25KD inhibited cell growth compared to the NC and PBS groups (Figure 3B). The results of the transwell and wound healing assays demonstrated that HSC-derived exosomes with high circWDR25 levels dramatically enhanced invasion by HCC cells compared to exosomes with low circWDR25 levels (Figure 3E-F). Collectively, these findings indicate that circWDR25 derived from HSC exosomes plays an oncogenic role in HCC cells.

3.4. CircWDR25 acts as a sponge for miR-4474-3p

Based on a cross-analysis of microRNA target prediction databases (TargetScan and miRanda), 298 miRNAs with potential binding sites for circWDR25 were identified (Table S6, *http://www.biosciencetrends.com/action/getSupplementalData.php?ID=109*). For instance, miR-4474-3p, miR-6856-5p, miR-889-5p, miR-210-5p, and miR-6763-5p were the most likely potential binding sites for circWDR25 (Figure 4A). Of note, circWDR25 had four binding sites with miR4474-3p (Figure 4B), and miR4474-3p was the most highly enriched miRNA in sponge complexes with circWDR25, a finding that was confirmed by pull-down assays with a biotin-labelled circWDR25 probe. In addition, FISH analysis of HEK293T cells indicated that circWDR25 was colocalized with miR-4474-3p in the cytoplasm (Figure 4C). Moreover, after a pull-down assay was performed with a biotinylated miR-4474-3p mimic, qRT-PCR revealed significant enrichment of circWDR25 compared to negative controls. Moreover, miR-4474-3p was the most highly enriched miRNA in the sponge complexes for hepatoma cells (Figure 4D). To further verify the specific binding region between circWDR25 and miR-4474-3p, a dual-luciferase reporter assay was performed in HEK293T cells. After cotransfecting HEK293T cells with miR-4474-3p mimics and a circWDR25-WT reporter gene, a miR-4474-3p mimic significantly reduced the luciferase activity of the circWDR25-WT

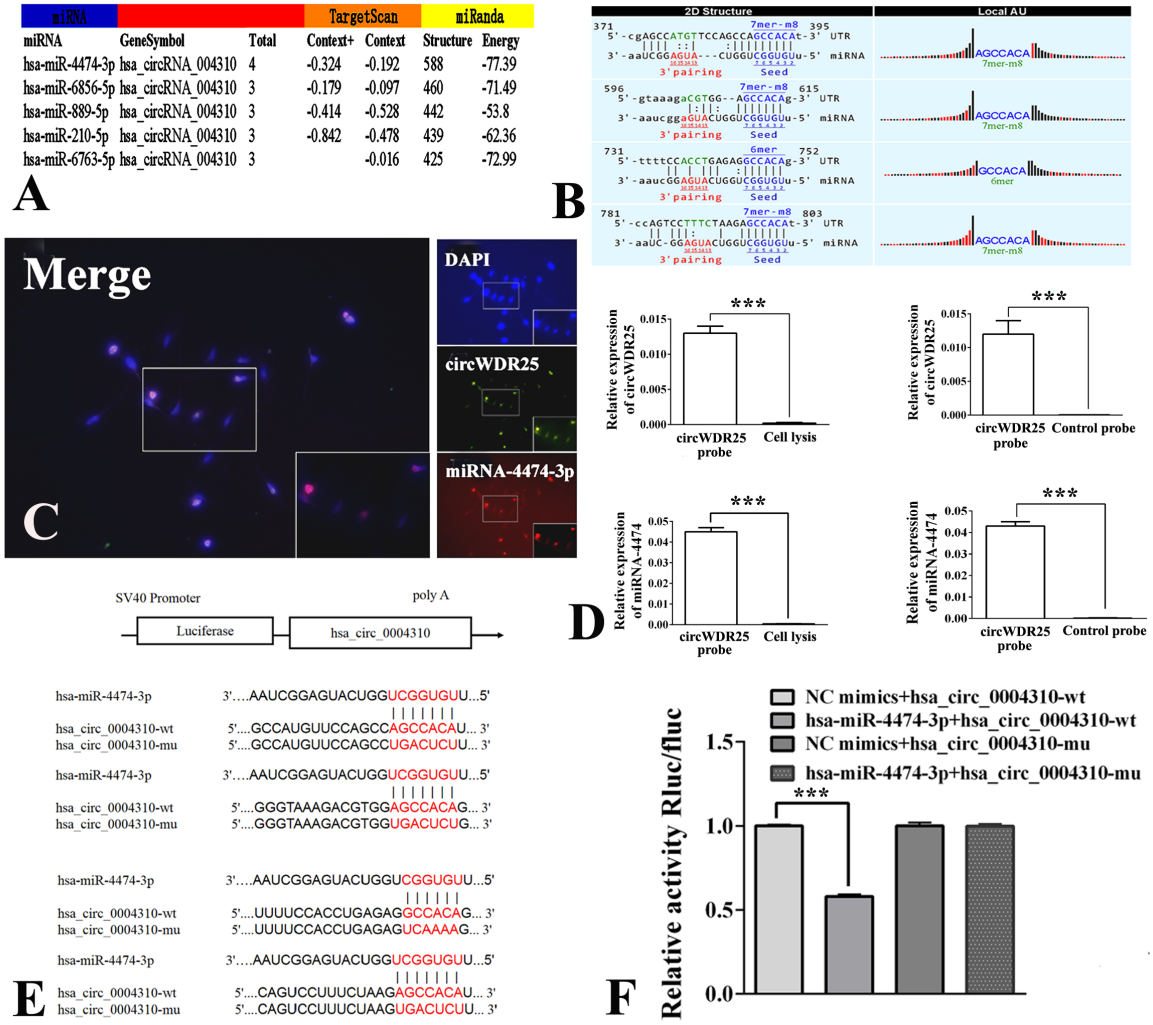

Figure 4. CircWDR25 functions as a sponge for miR-4474-3p. A: The top five target miRNAs with potential binding sites for circWDR25 as predicted by TargetScan and miRanda. **B:** The putative binding sites of miR-4474-3p in circWDR25. **C:** The colocalization of circWDR25 and miR-4474-3p in HEK293T cells was determined using a FISH assay. **D:** After a pull-down assay was performed with a biotinylated miR-4474-3p mimic, qRT–PCR indicated significant enrichment of circWDR25 compared to negative controls. **E-F:** The luciferase activity of the circWDR25 dual-luciferase reporter vector (WT or MUT) in HEK293T cells cotransfected with miR-4474-3p. All data are expressed as the mean ± SD of three independent experiments. $^{***}p < 0.001$.

reporter but not the mutant circWDR25 reporter (Figure 4E-F). Thus, circWDR25 acts as a sponge of miR-4474-3p and suppresses its expression.

3.5. MiR-4474-3p reverses the oncogenic effects of circWDR25 in HCC cells

MiR-4474-3p mimics were successfully transfected into HCC cells (Figure S2A, *http://www.biosciencetrends.com/action/getSupplementalData.php?ID=106*). The levels of miR-4474-3p expression in the two HCC cell lines decreased or increased after transfection with lentivirus carrying circWDR25OE or circWDR25KD, respectively (Figure S2B, *http://www.biosciencetrends.com/action/getSupplementalData.php?ID=106*). After transfecting miR-4474-3p mimics in HCC cells (Figures S2C and S3A, *http://www.biosciencetrends.com/action/getSupplementalData.php?ID=106*), CCK-8 assays, transwell assays, and wound healing assays indicated that cell proliferation, invasion, and migration decreased significantly (Figures 5A-B and S3A-D, *http://www.biosciencetrends.com/action/getSupplementalData.php?ID=106*). To further elucidate the functions of miR-4474-3p in circWDR25-induced signalling, rescue experiments were performed with cotransfection of miR-4474-3p mimics or miR-4474-3pNC with circWDR25OE or circWDR25NC. Promotion of the migration and invasion by HCC cells induced by circWDR25OE was reversed by miR-4474-3p mimics in transwell assays (Figures 5B and S3D, *http://www.biosciencetrends.com/action/getSupplementalData.php?ID=106*). These results suggest that miR-4474-3p has an anti-oncogenic effect on HCC cells and that it has an important function downstream of circWDR25.

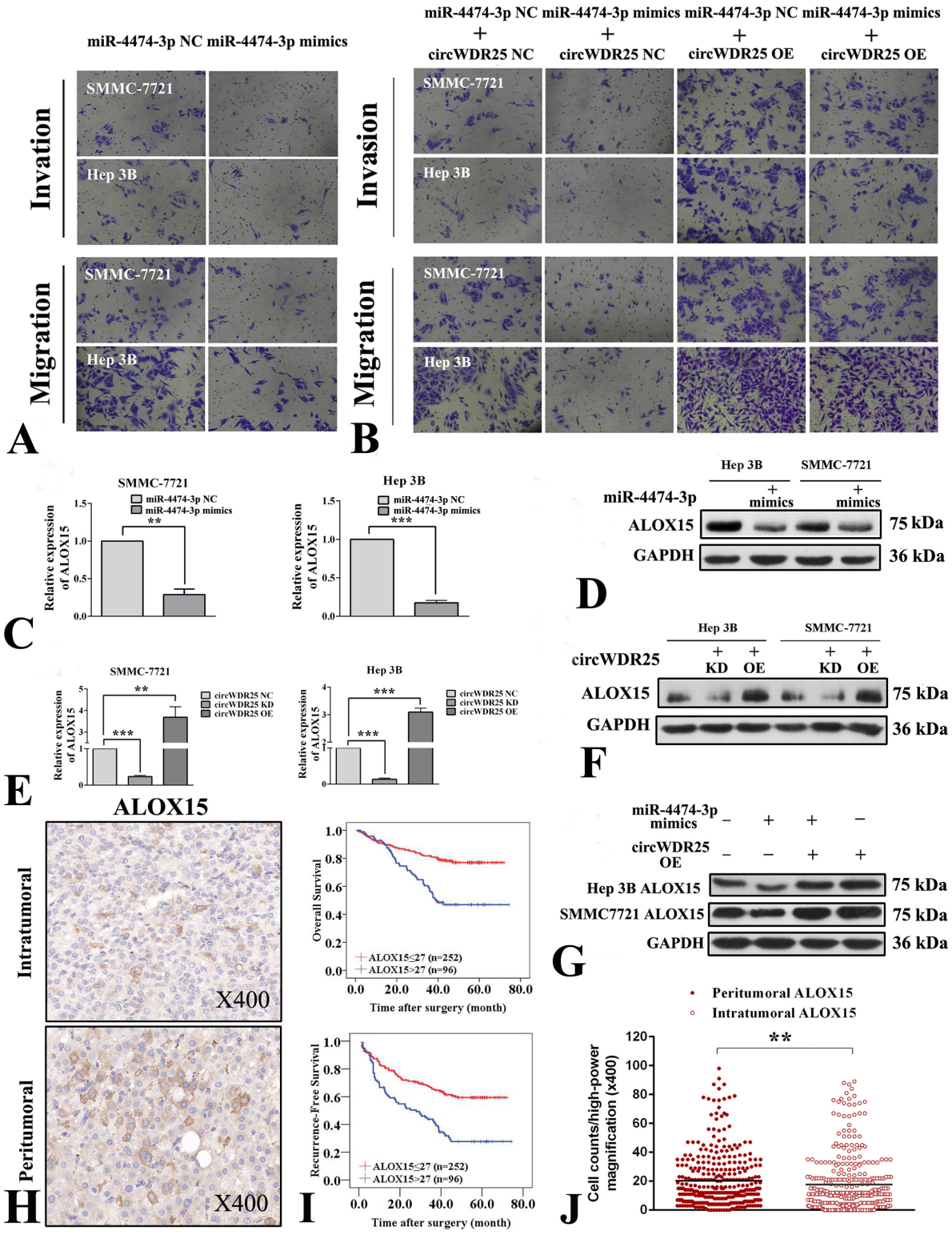

Figure 5. MiR-4474-3p reverses the oncogenic effects of circWDR25, which indirectly regulates ALOX15. A: Invasion and migration by HCC cells as were affected by the miR-4474-3p mimics were analyzed using a transwell assay. **B:** Transwell assays indicated that miR-4474-3p reversed the oncogenic effects of circWDR25 in four groups of HCC cells. **C-D:** qRT-PCR and western blot analyses of the relative levels of ALOX15 expression in HCC cells after transfection with the miR-432-5p mimics. **E-F:** The relative levels of ALOX15 mRNA and protein in HCC cells after transfection with the circWDR25KD or circWDR25OE. **G:** Western blot analyses of the relative levels of ALOX15 expression in HCC cells after transfection with the miR-432-5p mimics or/and circWDR25OE. **H:** IHC staining of intratumoral and peritumoral ALOX15 in patients with HCC (400× magnification). **I:** Kaplan-Meier survival curves showing the OS and RFS for peritumoral ALOX15 expression based on a tissue microarray including 348 patients with HCC. **J:** The scatter diagram showed that there were higher levels of ALOX15 expression in peritumoral liver tissues than in paired intratumoral tissues. All data are expressed as the mean ± SD of three independent experiments. $^{**}p < 0.01$, $^{***}p < 0.001$.

3.6. ALOX-15 is a downstream target of miR-4474-3p and is indirectly regulated by circWDR25

To further investigate the potential gene targets of miR-4474-3p and their underlying mechanism in HCC, the online programs TargetScan and miRDB were used to perform a bioinformatic analysis. According to the two databases, 435 and 3,851 predicted genes were possibly targeted by miR-4474-3p (Tables S7 and S8, *http://www.biosciencetrends.com/action/getSupplementalData.php?ID=107; http://www.biosciencetrends.com/action/getSupplementalData.php?ID=110*). Both of these databases indicated that ALOX15 had the highest prediction score and could be a downstream target of miR-4474-3p. The dual-luciferase reporter assay also demonstrated that a miR-4474-3p mimic significantly reduced the luciferase activity of the ALOX15 3′-UTR WT reporter but not the mutant ALOX15 3′-UTR reporter (Figure S4A-B, *http://www.biosciencetrends.com/action/getSupplementalData.php?ID=106*). Moreover, qRT–PCR and a Western blot analysis suggested that miR-4474-3p mimics negatively regulated the expression of ALOX15 in both cell lines (Figures 5C-D and S4C, *http://www.biosciencetrends.com/action/getSupplementalData.php?ID=106*). In addition, the levels of mRNA and protein expression for ALOX15 were positively regulated by circWDR25 (Figures 5E-F and S4D, *http://www.biosciencetrends.com/action/getSupplementalData.php?ID=106*). The effect of circWDR25OE was fully rescued by miR-4474-5p mimics (Figures 5G and S4E, *http://www.biosciencetrends.com/action/getSupplementalData.php?ID=106*). These results identified ALOX-15 as a downstream target of miR-4474-3p that was potentially indirectly regulated by circWDR25. Elucidation of the regulatory mechanism involved in this signal pathway depends partially on further investigation of the interaction between miR-4474-3p and ALOX15.

3.7. ALOX15 is associated with the prognosis for HCC

Clinically, since the current results indicated that circWDR25 acts as a predictor of the outcomes of HCC and to regulate the levels of ALOX15 expression, whether ALOX15 was associated with HCC progression was also assessed (Figure 5H-I). Inconsistent with the expression of circWDR25, the levels of ALOX15 expression were higher in peritumoral liver tissues than in paired intratumoral tissues (Figure 5H and 5J). However, similar to peritumoral circWDR25, both univariate analysis and multivariate analysis revealed that peritumoral ALOX15 could predict the OS and RFS for patients with HCC (Figure 5I). There was no correlation between ALOX15 and characteristics of patients with HCC (Table S9, *http://www.biosciencetrends.com/action/getSupplementalData.php?ID=107*). Together, the aforementioned results verify that the circWDR25-miR4474-3p-ALOX15 axis may contribute to the tumorigenesis and progression of HCC.

3.8. Exogenous and HSC exosome-derived circWDR25 induces an EMT

A previous study by the current authors found that activated HSC secretions facilitated the aggressiveness of HCC *via* an EMT (*13*). Here, whether the expression of EMT markers was regulated by the circWDR25-miR4474-3p pathway *in vitro* was further investigated. Exogenous circWDR25KD or miR-4474-3p mimics were found to increase the expression of E-cadherin but decrease the expression of vimentin in both HCC cell lines. CircWDR25OE was completely rescued by miR-4474-5p mimics (Figures 6C and S5E-F, *http://www.biosciencetrends.com/action/getSupplementalData.php?ID=106*). In addition, the EMT induced by HSC exosome-derived circWDR25 was examined in HCC cells. Similarly, *in vitro* HSC exosome-derived circWDR25KD or circWDR25OE had the same effects on the EMT pathways in both cell lines and positively regulated the level of expression of the downstream gene ALOX15 (Figures 6D and S5G-J, *http://www.biosciencetrends.com/action/getSupplementalData.php?ID=106*). *in vivo* xenograft mouse experiments indicated that exosomal circWDR25KD from HSCs promoted EMT in tumors induced by the two HCC cell lines, which downregulated the expression of E-cadherin, increased the expression of N-cadherin and vimentin, and upregulated ALOX15 expression (Figures 6E and S5K-N, *http://www.biosciencetrends.com/action/getSupplementalData.php?ID=106*). IHC staining for EMT markers in the subcutaneous tumor yielded the same results as Western blotting *in vivo* (Figures 6F and S5O, *http://www.biosciencetrends.com/action/getSupplementalData.php?ID=106*) and further confirmed the critical effects of exosomal circWDR25KD from HSCs on the EMT pathway.

3.9. CircWDR25 and ALOX15 synergistically regulate the expression of PD-L1 in hepatoma cells and CTLA-4 in HSCs

A previous study indicated that ALOX15 was upregulated in tumor-associated macrophages (TAMs) and that it promoted CTLA-4 expression in T lymphocytes (*34*). Moreover, the PD-L1 pathway that was involved in inducing tolerance was regulated by ALOX15 (*35*). Here, the ALOX-15 inhibitor PD146176 exhibited a dose-independent inhibitory effect on the expression of PD-L1 protein in HCC cells and it extenuated the influence of circWDR25OE transported by HSC exosomes (Figure 7A-C). After stimulation with LPS and coculturing with HSC-derived exosomal circWDR25OE, there was a significant increase in CTLA-4 expression in activated HSCs (Figure 7 D-F).

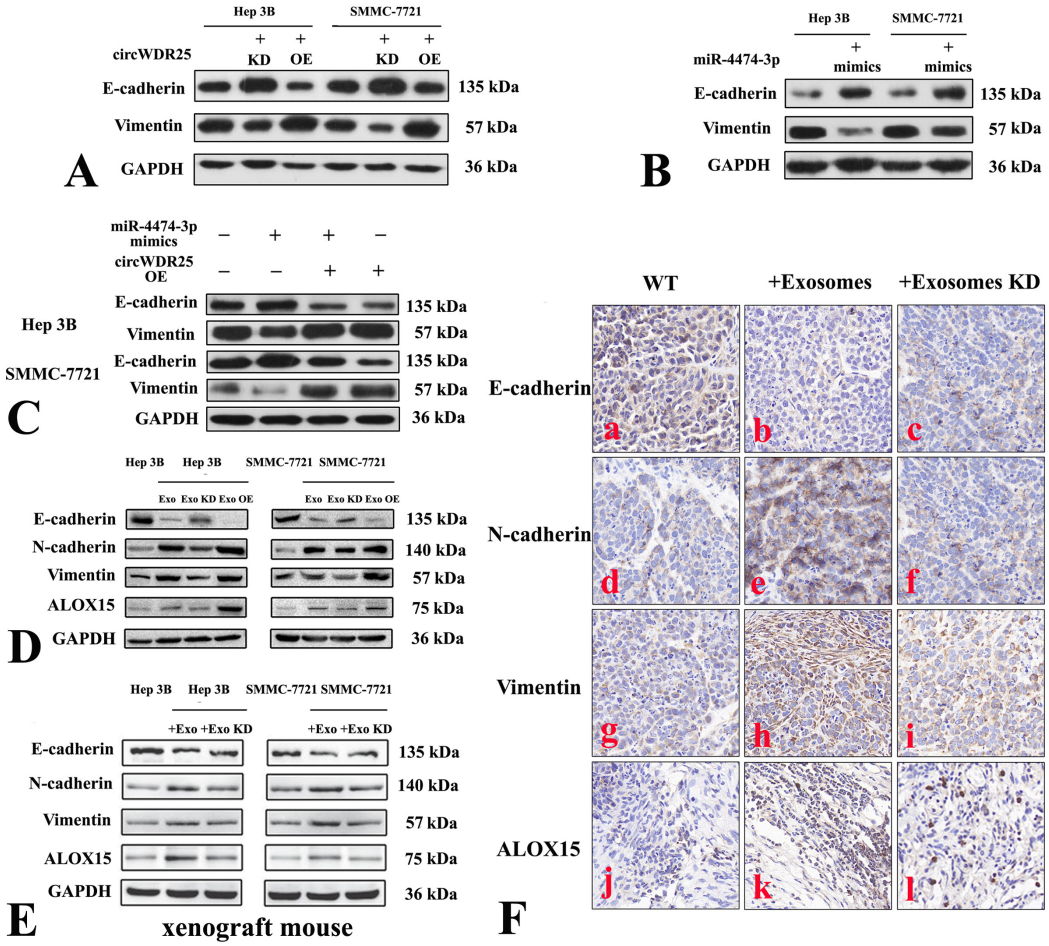

Figure 6. Exogenous and HSC exosome-derived circWDR25 induce epithelial-to-mesenchymal transition (EMT). A-B: The levels of expression of EMT marker proteins in HCC cells as were affected by circWDR25KD, circWDR25OE, or miR-4474-3p mimics were determined using Western blot analysis. **C:** The relative expression of EMT marker proteins in HCC cells as was affected by circWDR25KD, miR-4474-3p mimics, or a combination of the two. **D:** The levels of expression of EMT marker and ALOX15 proteins in HCC cells cultured with HSC-derived exosome circWDR25KD or circWDR25OE. **E:** The levels of expression of EMT marker and ALOX15 proteins in tumors of xenograft mice injected with HSC-derived exosomal circWDR25KD. **F:** Representative images of IHC staining of mouse tumors revealed the effects of exosomal circWDR25KD from HSCs on the EMT markers and ALOX15 (400× magnification).

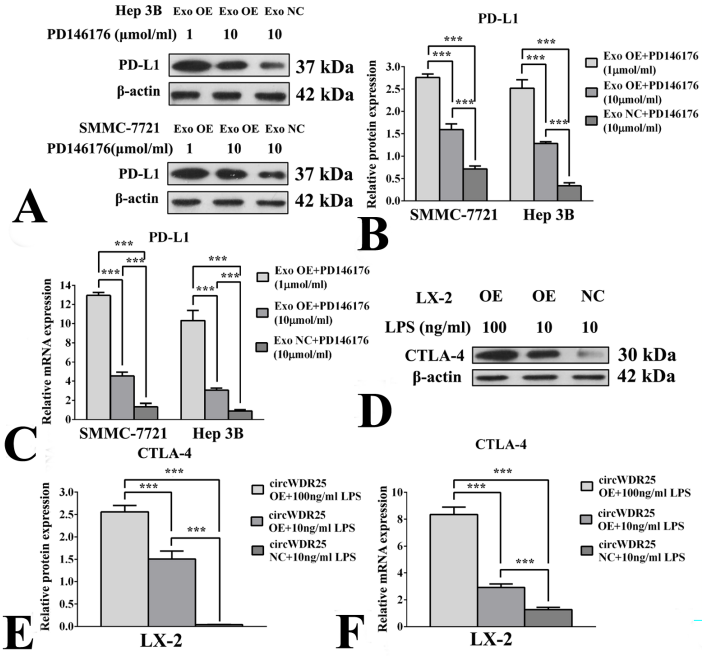

Figure 7. ALOX15 regulates the expression of PD-L1 in HCC cells and CTLA-4 in HSCs. A-B: Western blot analyses of the relative levels of expression of PD-L1 protein in HCC cells after treatment with exosome-derived circWDR25OE or circWDR25NC and different doses of the ALOX-15 inhibitor PD146176. **C:** qRT-PCR analyses of the relative levels of PD-L1 mRNA expression in HCC cells with the same treatments. **D-E:** Western blot analyses of the relative levels of expression of CTLA-4 protein in HSCs after stimulation with circWDR25OE or circWDR25NC and different doses of LPS. **F:** qRT-PCR analyses of the relative levels of CTLA-1 mRNA expression in HSCs with the same treatments. All data are expressed as the mean ± SD of three independent experiments. $^{***}p < 0.001$.

These data indicated that circWDR25 and ALOX-15 played potential synergistic roles in the immune response of the HCC microenvironment and that they might be therapeutic targets. Moreover, a daunting challenge would be to examine the immunotherapy effect of related drugs on HCC *via* this pathway.

4. Discussion

Emerging evidence indicates that in the tumor milieu of HCC, activated HSCs may accelerate the neoplastic transformation of hepatocytes after interactions with hepatocytes. The current study used RNA sequencing to profile circRNA expression in HSCs (LX-2) after stimulation with 3 different HCC cell lines (Hep3B, SMMC-7721, and HCCLM3), resulting in the identification of differentially expressed circRNAs. This study is the first to identify the circRNA hsa_circ_004310, designated circWDR25, as a significantly upregulated circRNA in tumor-activated HSCs and HCC tissues. Moreover, results indicated that HSC-secreted exosomal circWDR25 was delivered to HCC cells, it upregulated ALOX15 expression by sponging miR-4474-3p, and it in turn induced EMT. Moreover, loss- and gain-of-function experiments revealed that HSC-derived exosomal circWDR25 enhanced the proliferation and aggressiveness of HCC cells and facilitated the transmission of tumor information. The oncogenic role of circWDR25 was also corroborated by its potential prognostic value in patients with HCC. More importantly, results indicated that circWDR25-overexpressing HSCs and exosomal circWDR25-stimulating HCC cells were characterized by increased expression of CTLA-4 and PD-L1, respectively. All of the above results suggest that exosomal circWDR25 may provide a potential immunotherapy-related antitumor target for patients with HCC.

The current results indicated that circWDR25 was a critical signal transducer in the cellular network of the tumor microenvironment when preferentially exposed to cancer cells *via* the transport of HSC-derived exosomes. Many studies have confirmed that HCC development and progression are greatly influenced by dozens of circRNAs, which are enriched and stable in exosomes and can act in cellular networks. However, few studies have reported the role of HSC-derived exosomes in HCC. Most recently, Xia *et al*. (*24*) confirmed that HCC cell-derived exosomal smoothing promoted HCC progression after activating HSCs *via* the hedgehog pathway. Another recent study revealed that exosomes derived from HSCs stimulated cytokine synthesis-release and cell migration of macrophages and subsequently modulated the inflammatory response and fibrosis (*36*). The current study indicated that both HSC exosomal circWDR25 and also endogenous circWDR25 enhanced the proliferation of and invasion by HCC cells. Hence, circWDR25 acts as a bridging cytokine between HSC-to-HCC cell communications. In addition, these studies suggested its functional properties and triggering of hepatocarcinogenesis during the development of HCC.

Cytoplasmic exon circRNAs primarily function through miRNA sponging. Multiple-sequence alignment analyses have already revealed that miR-4474-3p is a microRNA target site of some exon and intron enhancers and silencers and transcription factors, some of which are cancer related (*37*). Cross-analysis of miRanda and TargetScan in the current study revealed that 4 miRNAs harbored potential binding sites for circWDR25. Of note, miR4474-3p was the most highly enriched miRNA in the sponge complexes with circWDR25, which was confirmed by pull-down assays with a circWDR25 probe. Dual-luciferase assays also verified the binding between circWDR25 and miR-4474-3p. The above results indicated that circWDR25 could directly bind to the seed region of miR-4474-3p in the cytoplasm of HCC cells. A rescue experiment to elucidate the biological function of this complex indicated that the circWDR25OE-induced enhancement of tumor proliferation and migration was reversed by treatment with miR-4474-3p mimics. Therefore, this study has demonstrated that circWDR25 functions as a miR-4474-3p sponge and that it has an effect on the proliferation of and invasion by HCC, and especially *via* transportation of HSC-derived exosomes.

As a target of miR-4474-3p, ALOX15 is upregulated in HCC cells and peritumoral tissues. Notably, ALOX15, an enzyme for lipid metabolism, has been widely reported to play important roles in a variety of human diseases, and especially oxidative stress, immune/inflammatory responses, and cancer (*38*). In HCC, Ma *et al*. found that ALOX15 prevented cancer cell apoptosis and promoted cancer cell growth and metastasis *via* the interaction of the Akt/heat shock protein (HSP)-90 pathway (*39*). The current study also indicated that circWDR25 promoted HCC progression *via* the circWDR25/miR-4474-3p/ALOX15 axis. Another important finding was that peritumoral ALOX15 serves as an unfavorable prognostic predictor in HCC. Given its involvement in inflammatory responses and the roles of the peritumoral inflammatory environment as the principal target of intrahepatic metastasis (*14,16*), ALOX15 may facilitate intrahepatic metastases, probably through the conversion of the proinflammatory response to tumor development.

Recently, EMT programs, a process involving a loss of epithelial cell polarity, extracellular matrix remodelling, and premetastatic niche formation, have garnered attention again due to emerging concepts and evidence related to cancer heterogeneity and metastasis (*40*). Oncogenic exosomal miRNAs (*e.g.*, miR-23a, miR-193a-3p, miR-210-3p, and miR-5100 (*41*)) and circRNAs (*e.g.*, circ-0004277 (*42*)) are also involved in the regulation of EMT. Similarly, the current findings suggest that HSC exosomal circWDR25 induces EMT in HCC *via* the miR4474-3p-ALOX15 axis. *In*

vitro experiments also verified that HSC exosomal and endogenous circWDR25 promoted migration and invasion by HCC cells. Taken together, these results provide evidence that circWDR25 can indirectly (HSC-derived exosomes) or directly (endogenously) enhance the progression of HCC metastasis *via* the EMT process.

Currently, the combination of immune checkpoint inhibitors (ICIs), such as PD-1 and CTLA-4, has efficacious synergistic antitumor activity and therefore has emerged as an anticancer strategy in HCC associated with high levels of their expression in tumor cells and immune cells, inducing T cell inhibition and tumor immune escape (*43*) . Interestingly, the current findings indicated that circWDR25 and ALOX15 can synergistically regulate the levels of CTLA-4 expression in HSCs or PD-L1 in HCC cells, possibly suggesting that the circWDR25-ALOX-15 signalling pathway is involved in immunomodulatory activity between activated HSCs and HCC cells. To date, tumor mutational burden (TMB) and PD-L1 expression are the most extensively studied predictive biomarkers of immunotherapy efficacy. The results for circWDR25 and ALOX15 in the current study indicated that they synergistically provoked the activation of the PD-L1 and CTLA-4 pathways and may have distinct but complementary effects in negatively regulating immune activity and as predictive biomarkers of the efficacy of immunotherapy. However, further studies need to explore the in-depth mechanisms.

The current study had several limitations. (*i*). Given the role of circWDR25 as an upstream gene in this signalling pathway, its regulatory mechanism involved miR-4474-3p-ALOX15. A regulatory relationship between miR-4474-3p and ALOX15 was identified, but the specific regulatory mechanism of miR-4474-3p on ALOX15 should be explored in the future. (*ii*) Further studies need to validate the immunotherapy efficacy of related drugs *via* this pathway, taking into consideration the complexity of signalling networks, the target drug combined with PD-1 or CTLA-4, medication dosage and duration of administration, and even the possibility of clinical trials. (*iii*) If gene knockout mice were available, more accurate and detailed evidence regarding drug treatment and the malignant capacity for invasion and metastasis induced by these oncogenes could be obtained.

In conclusion, circWDR25 was identified as a novel circRNA that is involved in the progression of HCC. To the extent known, few studies have examined the mechanism of exosomal circRNAs from HSCs in HCC.

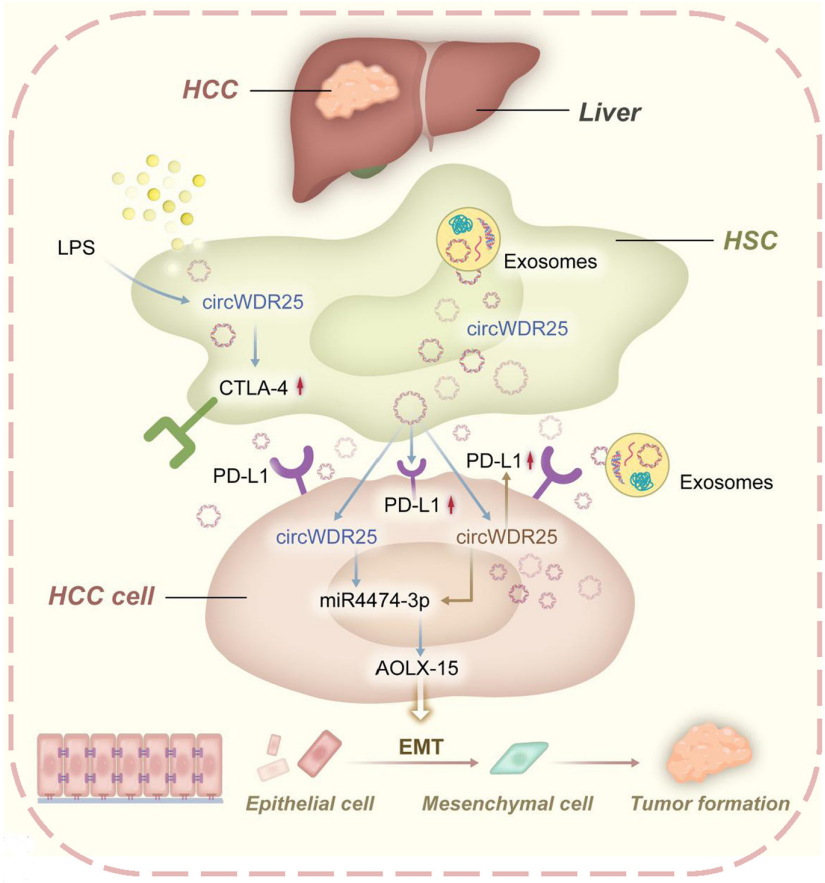

Figure 8. Diagram of the mechanistic findings. Exogenous and HSC exosome-derived circWDR25 promotes HCC cell proliferation, migration, and invasion through the circWDR25/miR-4474-3p/ALOX15 and epithelial-to-mesenchymal transition (EMT) axes. In addition, circWDR25 also increased the expression of PD-L1 in HCC and CTLA-4 in HSCs.

A valuable contribution of this study is the identification of the important role of HSC-derived exosomal circRNA (circWDR25) in cell-to-cell communications, which may be responsible for tumor aggressiveness *via* the downstream miR4474-3p/ALOX15 regulatory loop and EMT pathway in HCC. Importantly, both circWDR25 and ALOX15 were able to predict the outcomes of HCC and stimulate the expression of CTLA-4 and PD-L1 (Figure 8). In this regard, both may be promising predictive biomarkers of the prognosis for HCC and the efficacy of immunotherapy.

Funding: This work was supported by a grant from the National Natural Science Foundation of China (No. 82170666) and a Science and Health Joint Research Project of Chongqing City (2020GDRC013); CQMU Program for Youth Innovation in Future Medicine (W0087).

Conflict of Interest: The authors have no conflicts of interest to disclose.

References

1. Forner A, Reig M, Bruix J. Hepatocellular carcinoma. Lancet. 2018; 391:1301-1314.
2. Wen N, Cai Y, Li F, Ye H, Tang W, Song P, Cheng N. The clinical management of hepatocellular carcinoma worldwide: A concise review and comparison of current guidelines: 2022 update. Biosci Trends. 2022; 16:20-30.
3. Deng ZJ, Li L, Teng YX, Zhang YQ, Zhang YX, Liu HT, Huang JL, Liu ZX, Ma L, Zhong JH. Treatments of hepatocellular carcinoma with portal vein tumor thrombus: Current status and controversy. J Clin Transl Hepatol. 2022; 10:147-158.
4. Villanueva A. Hepatocellular Carcinoma. N Engl J Med. 2019; 380:1450-1462.
5. Yang JD, Hainaut P, Gores GJ, Amadou A, Plymoth A, Roberts LR. A global view of hepatocellular carcinoma: Trends, risk, prevention and management. Nat Rev Gastroenterol Hepatol. 2019; 16:589-604.
6. Qiu G, Xie K, Jin Z, Jiang C, Liu H, Wan H, Huang J. The multidisciplinary management of hepatocellular carcinoma with portal vein tumor thrombus. Biosci Trends. 2021; 15:148-154.
7. Tsuchida T, Friedman SL. Mechanisms of hepatic stellate cell activation. Nat Rev Gastroenterol Hepatol. 2017; 14:397-411.
8. Myojin Y, Hikita H, Sugiyama M, *et al*. Hepatic stellate cells in hepatocellular carcinoma promote tumor growth *via* growth differentiation factor 15 production. Gastroenterology. 2021; 160:1741-1754 e1716.
9. Xiao H, Zhang Y, Li Z, Liu B, Cui D, Liu F, Chen D, Liu Y, Ouyang G. Periostin deficiency reduces diethylnitrosamine-induced liver cancer in mice by decreasing hepatic stellate cell activation and cancer cell proliferation. J Pathol. 2021; 255:212-223.
10. Liu C, Zhou X, Long Q, Zeng H, Sun Q, Chen Y, Wu D, Liu L. Small extracellular vesicles containing miR-30a-3p attenuate the migration and invasion of hepatocellular carcinoma by targeting *SNAP23* gene. Oncogene. 2021; 40:233-245.
11. Kang MJ, Lee S, Jung U, Mandal C, Park H, Stetler-Stevenson WG, Kim YS, Moon JW, Park SH, Oh J. Inhibition of hepatic stellate cell activation suppresses tumorigenicity of hepatocellular carcinoma in mice. Am J Pathol. 2021.
12. Liao R, Sun TW, Yi Y, Wu H, Li YW, Wang JX, Zhou J, Shi YH, Cheng YF, Qiu SJ, Fan J. Expression of TREM-1 in hepatic stellate cells and prognostic value in hepatitis B-related hepatocellular carcinoma. Cancer Sci. 2012; 103:984-992.
13. Xie YX, Liao R, Pan L, Du CY. ERK pathway activation contributes to the tumor-promoting effects of hepatic stellate cells in hepatocellular carcinoma. Immunol Lett. 2017; 188:116-123.
14. Liao R, Wu H, Yi Y, Wang JX, Cai XY, He HW, Cheng YF, Zhou J, Fan J, Sun J, Qiu SJ. Clinical significance and gene expression study of human hepatic stellate cells in HBV related-hepatocellular carcinoma. J Exp Clin Cancer Res. 2013; 32:22.
15. Liao R, Sun J, Wu H, Yi Y, Wang JX, He HW, Cai XY, Zhou J, Cheng YF, Fan J, Qiu SJ. High expression of IL-17 and IL-17RE associate with poor prognosis of hepatocellular carcinoma. J Exp Clin Cancer Res. 2013; 32:3.
16. Zhou BY, Gong JH, Cai XY, Wang JX, Luo F, Jiang N, Gong JP, Du CY, Liao R. An imbalance between stellate cells and gammadeltaT cells contributes to hepatocellular carcinoma aggressiveness and recurrence. Hepatol Int. 2019; 13:631-640.
17. Kalluri R, LeBleu VS. The biology, function, and biomedical applications of exosomes. Science. 2020; 367:eaau6977.
18. Morrissey SM, Zhang F, Ding C, *et al*. Tumor-derived exosomes drive immunosuppressive macrophages in a pre-metastatic niche through glycolytic dominant metabolic reprogramming. Cell Metab. 2021;33:2040-2058.e10.
19. Jiang C, Zhang N, Hu X, Wang H. Tumor-associated exosomes promote lung cancer metastasis through multiple mechanisms. Mol Cancer. 2021; 20:117.
20. Wu J, Gao W, Tang Q, *et al*. M2 macrophage-derived exosomes facilitate HCC metastasis by transferring alphaM beta2 integrin to tumor cells. Hepatology. 2021; 73:1365-1380.
21. Shefler I, Salamon P, Mekori YA. Extracellular vesicles as emerging players in intercellular communication: Relevance in mast cell-mediated pathophysiology. Int J Mol Sci. 2021; 22.
22. Herrera M, Llorens C, Rodriguez M, *et al*. Differential distribution and enrichment of non-coding RNAs in exosomes from normal and cancer-associated fibroblasts in colorectal cancer. Mol Cancer. 2018; 17:114.
23. Muralikumar M, Manoj Jain S, Ganesan H, A KD, Pathak S, Banerjee A. Current understanding of the mesenchymal stem cell-derived exosomes in cancer and aging. Biotechnol Rep (Amst). 2021; 31:e00658.
24. Xia Y, Zhen L, Li H, Wang S, Chen S, Wang C, Yang X. MIRLET7BHG promotes hepatocellular carcinoma progression by activating hepatic stellate cells through exosomal SMO to trigger Hedgehog pathway. Cell Death Dis. 2021; 12:326.
25. Zhou Y, Ren H, Dai B, Li J, Shang L, Huang J, Shi X. Hepatocellular carcinoma-derived exosomal miRNA-21 contributes to tumor progression by converting hepatocyte stellate cells to cancer-associated fibroblasts. J Exp Clin

Cancer Res. 2018; 37:324.
26. Liao R, Liu L, Zhou J, Wei X, Huang P. Current molecular biology and therapeutic strategy status and prospects for circRNAs in HBV-associated hepatocellular carcinoma. Front Oncol. 2021; 11:697747.
27. Shi L, Liu B, Shen DD, *et al*. A tumor-suppressive circular RNA mediates uncanonical integrin degradation by the proteasome in liver cancer. Sci Adv. 2021; 7:eabe5043.
28. Bu FT, Zhu Y, Chen X, Wang A, Zhang YF, You HM, Yang Y, Yang YR, Huang C, Li J. Circular RNA circPSD3 alleviates hepatic fibrogenesis by regulating the miR-92b-3p/Smad7 axis. Mol Ther Nucleic Acids. 2021; 23:847-862.
29. Costa-Silva B, Aiello NM, Ocean AJ, *et al*. Pancreatic cancer exosomes initiate pre-metastatic niche formation in the liver. Nat Cell Biol. 2015; 17:816-826.
30. Hao TT, Liao R, Lei DL, Hu GL, Luo F. Inhibition of B7-H4 promotes hepatocellular carcinoma cell apoptosis and autophagy through the PI3K signaling pathway. Int Immunopharmacol. 2020; 88:106889.
31. Zhang PF, Wei CY, Huang XY, Peng R, Yang X, Lu JC, Zhang C, Gao C, Cai JB, Gao PT, Gao DM, Shi GM, Ke AW, Fan J. Circular RNA circTRIM33-12 acts as the sponge of MicroRNA-191 to suppress hepatocellular carcinoma progression. Mol Cancer. 2019; 18:105.
32. Wang L, Long H, Zheng Q, Bo X, Xiao X, Li B. Circular RNA circRHOT1 promotes hepatocellular carcinoma progression by initiation of NR2F6 expression. Mol Cancer. 2019; 18:119.
33. Galon J, Costes A, Sanchez-Cabo F, *et al*. Type, density, and location of immune cells within human colorectal tumors predict clinical outcome. Science. 2006; 313:1960-1964.
34. Daurkin I, Eruslanov E, Stoffs T, Perrin GQ, Algood C, Gilbert SM, Rosser CJ, Su LM, Vieweg J, Kusmartsev S. Tumor-associated macrophages mediate immunosuppression in the renal cancer microenvironment by activating the 15-lipoxygenase-2 pathway. Cancer Res. 2011; 71:6400-6409.
35. Leconet W, Petit P, Peraldi-Roux S, Bresson D. Nonviral delivery of small interfering RNA into pancreas-associated immune cells prevents autoimmune diabetes. Mol Ther. 2012; 20:2315-2325.
36. Benbow JH, Marrero E, McGee RM, Brandon-Warner E, Attal N, Feilen NA, Culberson CR, McKillop IH, Schrum LW. Hepatic stellate cell-derived exosomes modulate macrophage inflammatory response. Exp Cell Res. 2021; 405:112663.
37. Dvorak P, Leupen S, Soucek P. Functionally significant features in the 5' untranslated region of the ABCA1 gene and their comparison in vertebrates. Cells. 2019; 8:623.
38. Orafaie A, Matin MM, Sadeghian H. The importance of 15-lipoxygenase inhibitors in cancer treatment. Cancer Metastasis Rev. 2018; 37:397-408.
39. Ma J, Zhang L, Zhang J, Liu M, Wei L, Shen T, Ma C, Wang Y, Chen Y, Zhu D. 15-lipoxygenase-1/15-hydroxyeicosatetraenoic acid promotes hepatocellular cancer cells growth through protein kinase B and heat shock protein 90 complex activation. Int J Biochem Cell Biol. 2013; 45:1031-1041.
40. Lambert AW, Weinberg RA. Linking EMT programmes to normal and neoplastic epithelial stem cells. Nat Rev Cancer. 2021; 21:325-338.
41. Liu J, Ren L, Li S, Li W, Zheng X, Yang Y, Fu W, Yi J, Wang J, Du G. The biology, function, and applications of exosomes in cancer. Acta Pharm Sin B. 2021; 11:2783-2797.
42. Zhu C, Su Y, Liu L, Wang S, Liu Y, Wu J. Circular RNA hsa_circ_0004277 stimulates malignant phenotype of hepatocellular carcinoma and epithelial-mesenchymal transition of peripheral cells. Front Cell Dev Biol. 2020; 8:585565.
43. Yau T, Kang YK, Kim TY, *et al*. Efficacy and safety of nivolumab plus ipilimumab in patients with advanced hepatocellular carcinoma previously treated with sorafenib: The CheckMate 040 Randomized Clinical Trial. JAMA Oncol. 2020; 6:e204564.

Received June 25, 2022; Revised July 27, 2022; Accepted August 3, 2022.

[§]These authors contributed equally to this work.
**Address correspondence to:*
Rui Liao, Department of Hepatobiliary Surgery, the First Affiliated Hospital of Chongqing Medical University, Chongqing 400016, China.
E-mail: liaorui99@163.com

Released online in J-STAGE as advance publication August 7, 2022.